Testosterone Inhibits Adipogenic Differentiation in 3T3-L1 Cells: Nuclear Translocation of Androgen Receptor Complex with β-Catenin and T-Cell Factor 4 May Bypass Canonical Wnt Signaling to Down-Regulate Adipogenic Transcription Factors

Rajan Singh, **Jorge N. Artaza**, **Wayne E. Taylor**, **Melissa Braga**, **Xin Yuan**, **Nestor F. Gonzalez-Cadavid**, and **Shalender Bhasin**

Division of Endocrinology, Metabolism, and Molecular Medicine (R.S., J.N.A., W.E.T., M.B., N.F.G.-C., S.B.), Charles R. Drew University of Medicine and Science, Los Angeles, California 90059; Beth Israel Deaconess Medical Center and Harvard Medical School (X.Y.), Boston, Massachusetts 02215; and Section of Endocrinology, Diabetes, and Nutrition (S.B.), Boston Medical Center, Boston, Massachusetts 02118

Abstract

Testosterone supplementation in men decreases fat mass; however, the mechanisms by which it inhibits fat mass are unknown. We hypothesized that testosterone inhibits adipogenic differentiation of preadipocytes by activation of androgen receptor (AR)/β-catenin interaction and subsequent translocation of this complex to the nucleus thereby bypassing canonical Wnt signaling. We tested this hypothesis in 3T3-L1 cells that differentiate to form fat cells in adipogenic medium. We found that these cells express AR and that testosterone and dihydrotestosterone dose-dependently inhibited adipogenic differentiation as analyzed by Oil Red O staining and down-regulation of CCAAT/enhancer binding protein-α and -δ and peroxisome proliferator-activated receptor-$\gamma2$ protein and mRNA. These inhibitory effects of androgens were partially blocked by flutamide or bicalutamide. Androgen treatment was associated with nuclear translocation of β-catenin and AR. Immunoprecipitation studies demonstrated association of β-catenin with AR and T-cell factor 4 (TCF4) in the presence of androgens. Transfection of TCF4 cDNA inhibited adipogenic differentiation, whereas a dominant negative TCF4 cDNA construct induced adipogenesis and blocked testosterone's inhibitory effects. Our gene array analysis indicates that testosterone treatment led to activation of some Wnt target genes. Expression of constitutively activated AR fused with VP-16 did not inhibit the expression of CCAAT/enhancer binding protein-α in the absence of androgens. Testosterone and dihydrotestosterone inhibit adipocyte differentiation *in vitro* through an AR-mediated nuclear translocation of β-catenin and activation of downstream Wnt signaling. These data provide evidence for a regulatory role for androgens in inhibiting adipogenic differentiation and a mechanistic explanation consistent with the observed reduction in fat mass in men treated with androgens.

Address all correspondence and requests for reprints to: Rajan Singh, Ph.D., Division of Endocrinology, Metabolism, and Molecular Medicine, Charles R. Drew School of Medicine, 1731 East 120th Street, Augustus F. Hawkins Building, Los Angeles, California 90059. rajansingh@mednet.ucla.edu..

After decades of intense controversy, a consensus has emerged that androgens are important regulators of fat mass and distribution in mammals. Androgen-deficient men have higher fat mass than eugonadal controls. Experimentally induced androgen or androgen receptor (AR) deficiency is associated with gains in fat mass and a loss of fat-free mass (1, 2). Testosterone supplementation decreases fat mass in hypogonadal men and older men with low testosterone concentrations; these effects of testosterone on fat mass are correlated with testosterone dose and circulating concentrations (3–7). These observations of androgen effects on body composition have formed the rationale for clinical trials of testosterone supplementation in HIV-infected men with weight loss or fat redistribution syndrome (8, 9). There is evidence in rodents that high androgen levels modulate the proliferation and differentiation of preadipocytes differently in specific fat depots (10). Testosterone and dihydrotestosterone (DHT) treatment of epididymal preadipocytes *in vitro* inhibits the activity of glyceraldehyde-3-phosphate dehydrogenase (GAPDH), an adipose-specific enzyme (11). Testosterone also suppresses lipoprotein lipase (LPL) activity and lipid uptake in adipocytes (12). Rats with high androgens have impaired preadipocyte conversion to fat cells involving modulation of the CCAAT/enhancer binding protein (C/EBP) transcription factors (10). However, the mechanisms by which testosterone decreases fat mass are still poorly understood (13–16)

Androgens bind to AR, which mediates most of its physiological functions through transcriptional activation of downstream genes (17–20). AR has been detected in human and rat preadipocytes and adipocytes where it may be involved in regulating proliferation and differentiation of preadipocytes or pluripotent cells (2, 17, 18, 21). In addition, Ramirez *et al.* (12) have shown that androgen treatment of fully differentiated fat cells can inhibit expression of LPL and GAPDH to reduce fat mass. In addition, it has been suggested that androgens elicit antiadipogenic effects in the adipose precursor cells in specific regions where AR is expressed at a high level (17, 18). Adult male AR knockout mice exhibit a pseudofemale phenotype, and they have greater amounts of body fat than wild-type, male littermates (2, 22). These AR knockout mice are testosterone resistant, and they become obese and gain weight in sc and ip white adipose tissues (2). These studies suggest that AR may serve as a negative regulator of adipocyte development. Recently, it has been reported by various groups that AR interacts with β-catenin protein in the Wnt pathway in various cell lines (23–26). However, it is not known whether antiadipogenic effects of androgens are mediated through the downstream Wnt signaling pathway.

The Wnt gene family implicated in the control of adipo-genesis includes over 16 Wnt proteins, soluble secreted glycoproteins that signal through their frizzled receptors and have profound effects on cellular differentiation and growth (27–35). Activation of Wnt signaling inhibits glycogen synthase kinase 3β and allows cytosolic β-catenin to accumulate and translocate to the nucleus where it binds to the T-cell factor (TCF)/lymphoid-enhancer factor (LEF) family of transcription factors and activates transcription of Wnt-regulated target genes. In the absence of Wnt signaling, glycogen synthase kinase 3β phosphorylates β-catenin and targets it for ubiquitin-mediated degradation. MacDougald's group (35, 36) has demonstrated that Wnt signaling functions as an adipogenic switch that represses adipogenesis when activated and initiates adipogenesis when it is turned off. These

investigators reported that Wnt signaling, possibly mediated by Wnt 10b, maintains preadipocytes in an undifferentiated state through activation of β-catenin and TCF4, leading to subsequent inhibition of two well-characterized, key adipogenic transcription factors, C/EBP-α and peroxisome proliferator-activated receptor-γ (PPAR-γ), which are necessary and sufficient for adipogenic differentiation (35, 37, 38). Overexpression of dominant negative TCF4 (Dn-TCF4), which disrupts Wnt signaling, stimulates preadipocyte differentiation into mature adipocytes, whereas activation of Wnt signaling through TCF4 by lithium chloride blocks fat cell differentiation (35).

The role of the Wnt signaling pathway in mediating androgen effects on adipogenic differentiation has not been investigated. Although AR interacts with β-catenin protein in the Wnt pathway in some biological systems (23–26), the biological relevance of AR and β-catenin interaction is not fully understood. We considered the possibility that AR cross-talk and interaction with β-catenin/TCF may bypass canonical Wnt signaling to modulate adipogenic differentiation by directly activating downstream Wnt effector molecules including TCF/LEF.

We hypothesized that testosterone and DHT, the two potent androgens, inhibit adipogenic differentiation of preadipocytes by molecular mechanisms that involve AR and β-catenin interaction and modulation of downstream Wnt signaling through activation of TCF4. We tested this hypothesis in a 3T3-L1 cell line that has been used widely to investigate the mechanisms of preadipocyte differentiation; these cells, when grown in appropriate culture conditions, differentiate into adipocytes and recapitulate many of the endocrine and metabolic functions of mature adipocytes *in vivo* (39). We evaluated the expression of AR protein and mRNA in 3T3-L1 cells and determined the effects of testosterone and DHT on preadipocyte differentiation. We investigated the possible involvement of downstream effecter molecules in the Wnt signaling pathway by studying AR-β-catenin interaction and β-catenin nuclear translocation, a hallmark of Wnt activation, and determined the effects of TCF4 and Dn-TCF4 overexpression on inhibition of adipogenic differentiation by testosterone. We constitutively expressed AR-VP16 and investigated its effect on the adipogenic differentiation in this cell line, in the absence of androgens or nuclear β-catenin, to determine whether androgen-induced inhibition of adipo-genesis is mediated through AR binding to androgen response elements (AREs) in the promoter DNA or through TCF4/LEF DNA binding sites. We observed that constitutively expressed AR induced the protein expression of p21, which contains ARE binding sites in the promoter region (40); however, C/EBP-α level remained unchanged and β-catenin expression was not detected in the nucleus in 3T3-L1 cells.

Materials and Methods

Cell culture

Mouse 3T3-L1 preadipocytes (American Type Culture Collection, Manassas, VA) (passage 3–7) were maintained in growth medium (GM) containing DMEM supplemented with 10% fetal bovine serum (FBS) as described previously (41). Differentiation was induced in 100% confluent 3T3-L1 cells by incubating them in adipogenic medium (AM) (0.5 m$_M$ isobutylmethylxanthine, 1 μ_M dexamethasone, and 10 μg/ml insulin in GM) for 2 d with or

without androgens, followed by changing the medium to GM containing 10 μg/ml insulin with or without androgens at various concentrations for another 9–12 d. In some experiments, these cells were treated with AR antagonist flutamide or bicalutamide. The medium was changed every 2–3 d and replaced by fresh medium containing same concentrations of androgens.

Oil Red O staining

3T3-L1 cells were fixed in 2% paraformaldehyde after various treatments and stained with 0.5% Oil Red O (Sigma Chemical Co., Saint Louis, MO) for 15 min as described previously (36). For quantitative analysis of Oil Red O retention in these cells, stained adipocytes were extracted with 1 ml of 4% Igepal CA-630 (Sigma) in isopropanol, and absorbance was measured by spectrophotometry at 520 nm.

Western blot analysis

Cell lysates (50–100 μg) in lysis buffer (20 m$_M$ Tris, 0.5% SDS containing protease inhibitors) were subjected to Western blot analyses by 7.5–12% SDS-PAGE, using 1:500 dilutions of anti-C/EBP-β, anti-C/ EBP-δ, and anti-AR antibodies; 1:1000 anti-PPAR-γ; 1:300 anti-C/EBP-α; 1: 500 anti-p21; or 1:5000 anti-GAPDH antibody (Santa Cruz Biotechnology, Santa Cruz, CA). The washed filters were incubated with 1:2000 dilution of secondary antibodies linked to horseradish peroxidase. Immunoreactive bands were visualized by using the ECL detection system (Amersham Biosciences, Piscataway, NJ).

Quantitating adipogenic and Wnt target gene mRNA expression by RT-PCR and real-time quantitative PCR

Total RNA was extracted by using Trizol reagent, and equal amounts (2 μg) of RNA was reverse transcribed using RNA PCR kit (Applied Biosystems, Foster City, CA). The locations of forward/reverse PCR primers for real-time RT-PCR are as follows: AR (187 bp), 1937–1958/ 2124–2102 on S56585; GAPDH (152 bp), 606–626/758–738 on BC023196; PPAR-γ2 (241 bp), 79–99/320–299 on BC021798; C/EBP-α (225 bp), 843–864/1067–1047 on NM_007678; LEF1 (132 bp), 1539–1558 /1661– 1643 on NM_010703.2; and fatty acid binding protein 2 (AP2) (178 bp), 221–237/399–383 on K02109. The primers for PPAR-γ2 are specific for PPAR-γ2 and do not detect PPAR-γ1. Mouse gene PCR primer sets (RT[2]) were purchased from SuperArray Bioscience (Frederick, MD) for CD44 (183 bp), PPM03628A on NM_009851; and follistatin (Fst) (150 bp), PPM04451A on NM_008046. The QIAGEN Sybr Green PCR kit with HotStar *Taq* DNA polymerase was used (QIAGEN, Valencia, CA) with i-Cycler PCR thermocycler and fluorescent detector lid (Bio-Rad, Hercules, CA). The protocol includes melting for 15 min at 95 C, 40 cycles of three-step PCR including melting for 15 sec at 95 C, annealing for 30 sec at 58 C, elongation for 30 sec at 72 C with an additional detection step of 15 sec at 81 C, followed by a melting curve from 55–95 C at the rate of 0.5 C per 10 sec; except that for primers Fst, CD44, and LEF1, annealing was at 55 C and detection was at 76 C. We confirmed that inverse derivatives of melting curves show sharp peaks for PPAR-γ2 at 83.5 C, C/EBP-α at 88 C, AP2 at 84 C, CD44 at 84.5 C, LEF1 at 85.5 C, Fst at 84.5 C, and GAPDH at 87 C, indicating the correct products. Samples of 25 ng cDNA were analyzed in

quadruplicate in parallel with GAPDH controls; standard curves (threshold cycle *vs.* log pg cDNA) were generated by log dilutions of from 0.1 pg to 100 ng standard cDNA (reverse-transcribed mRNA from 3T3-L1 in AM), and then experimental mRNA starting quantities were calculated from the standard curves and averaged using i-Cycler, iQ software as described previously (21). The ratios of marker experimental gene (*e.g.* PPAR-γ2 mRNA) to GAPDH mRNA were computed and normalized to control (untreated) samples as 100%.

SuperArray analysis of Wnt target genes

Total cellular RNA isolated from 3T3-L1 cells undergoing adipogenic differentiation for 48 h with or without testosterone (100 n$_M$) treatment was subjected to cDNA gene array (GEArray Q Series, MM-043; SuperArray BioScience) analysis. This series of mouse Wnt signaling pathway gene array is designed to study the genes involved in and downstream of Wnt signaling. Biotin-labeled cDNA probes were synthesized from total RNA, denatured, and hybridized overnight at 60 C in GEHybridization solution to membranes spotted with Wnt signaling pathway-specific genes. Membranes were washed, and chemiluminescent analysis was performed as per the manufacturer's instructions. Raw data were analyzed using GEArray Expression Analysis Suite (SuperArray), and fold changes in relative gene expression were presented after background correction and normalization with a housekeeping gene.

Detection of AR, β-catenin, and adenomatous polyposis coli (APC) by immunofluorescence

3T3-L1 cells treated with or without testosterone for various time points were grown in 10% FBS in DMEM on eight-well chamber slides and fixed in 2% paraformaldehyde for 20 min, and for AR and APC assay, they were blocked with normal goat serum and incubated with rabbit anti-AR antibody (N20; Santa Cruz Biotechnology) at 1:50 dilution or rabbit anti-APC (N15; Santa Cruz Biotechnology) at 1:300 dilution. For β-catenin, the blocking step was done with normal horse serum followed by incubation with a monoclonal antibody against β-catenin (C19220; BD Biosciences PharMingen, San Diego, CA) at 1:500 dilutions. The detection of AR and APC was done with a 1:200 dilution of antirabbit biotinylated secondary antibody (Calbiochem, La Jolla, CA) or for β-catenin with antimouse biotinylated secondary antibody followed by streptavidin-fluorescein isothiocyanate (FITC) or Texas Red (Vector Laboratories, Burlingame, CA). After several washes, the slides were counterstained with 4',6-diamidino-2-phenyl-indole (DAPI) and mounted in prolong fade (Molecular Probes, Eugene, OR) and were examined under a fluorescence microscope equipped with the appropriate filters (42).

Double-labeling immunodetection of AR and β-catenin

The double localization of AR and β-catenin was carried out on 3T3-L1 cells treated with or without testosterone for various time points grown in 10% FBS in DMEM on eight-well chamber slides and fixed in 2% paraformaldehyde for 20 min. For AR, cells were blocked with normal goat serum and incubated with rabbit anti-AR antibody (N20; Santa Cruz Biotechnology) at 1:50 dilution, followed by a 1:200 dilution of antirabbit biotinylated secondary antibody (Calbiochem). The subsequent reaction was carried out by incubating

the cells in a 20-μg/ml solution of streptavidin-FITC (Vector), followed by 10% normal horse serum and then a 1:500 dilution of anti-β-catenin monoclonal antibody. Fluorescence labeling was performed with secondary antibody linked to Texas Red. The slides were counterstained with DAPI and mounted in prolong fade (Molecular Probes) and were examined under a fluorescence microscope equipped with the appropriate filters (42).

Cell fractionation and Western blot analysis to analyze β-catenin nuclear translocation

3T3-L1 cells treated with androgens (100 n_M testosterone and 10 n_M DHT) for 0–24 h, harvested, and separated into cytoplasmic and nuclear fractions using the nuclear and cytoplasmic extraction reagent (Pierce, Rockford, IL). Nuclear and cytoplasmic fractions (20–40 μg) were separated on 10% SDS-PAGE, and proteins were transferred onto polyvinylidene difluoride membrane (Amersham). Membranes were blocked with 5% nonfat milk in 0.05% Tween 20 in PBS for 1 h and incubated with β-catenin primary antibody (1:500 dilutions, C19220) for 2 h at room temperature. Detection of immunoreactive bands was achieved with antimouse-horseradish peroxidase-linked secondary antibody (Santa Cruz Biotechnology; sc-2031) and ECL detection reagents (Amersham; RPN 2106). The purity of nuclear and cytoplasmic fractions was assessed (data not shown) by using known cytoplasmic (hsp90) and nuclear (oct1) proteins.

Immunoprecipitation and immunoblot analysis to detect AR, β-catenin, and TCF4 interactions

The interactions between AR, β-catenin, and TCF4 were studied by immunoprecipitation. Cells were lysed using lysis buffer containing 20 m_M Tris-HCl (pH 7.8), 0.5% Nonidet P-40, 137 m_M NaCl, 50 μ_M EDTA, and protease inhibitors (Roche Diagnostics, Mannheim, Germany). Cell lysates were passed through a 30.5-gauge needle to disrupt nuclei. Protein extracts (500 μg) were incubated with either anti-AR (N20; Santa Cruz Biotechnology) or anti-TCF4 (Santa Cruz Biotechnology; Upstate, Charlottesville, VA) antibodies overnight at 4 C, followed by 1 h incubation with protein A/G-Sepharose (Calbiochem). Control immunoprecipitations were performed with rabbit preimmune serum. After three washes with 0.5 ml lysis buffer, the pellets were suspended in SDS sample buffer, boiled for 5 min, and analyzed on 10% SDS-PAGE. Proteins were transferred to a polyvinylidene difluoride membrane and blotted with anti-β-catenin, anti-AR, or anti-TCF4 antibodies.

Transient transfection and overexpression of full-length TCF4 and dominant-negative TCF4 (Dn-TCF4)

Full-length TCF4 cDNA and Dn-TCF4 cDNA constructs were kindly provided by Dr. M. Wierman (VA Medical, Denver, CO) and Dr. Eric Fearon (University of Michigan, Ann Arbor, MI), respectively. The Dn-TCF4 clone lacks 31 amino acids from the N terminus (TCF4 N31) and has been used successfully in previous studies to inhibit TCF function using a retroviral expression system (35, 36). However, we employed a transient transfection system using Lipofectamine 2000 (Invitrogen, Carlsbad, CA) with approximately 35–40% efficiency.

Transfection of constitutively active pAct-AR and dual luciferase assay

3T3-L1 cells were transfected with plasmids encoding full-length AR fused to VP16 activation domain (pAct-AR), ARE-promoter-luciferase (pARE$_4$-Luc), and empty pGL3 vectors either transfected alone or in combination using Lipofectamine 2000 with standard protocols. Cells were allowed to differentiate in adipogenic conditions for 9 d, and C/EBP-α mRNA and protein levels were analyzed. As a control for endogenous AR-responsive gene, we measured the expression of p21 after transfection of 3T3-L1 cells with pARE$_4$-Luc and pAct-AR vectors. The transfection efficiency in these experiments was measured both by immunostaining of the transfected cells with hemaglutinin (HA) antibody as well as by parallel transfection using GFP vector. Our transfection efficiency under these conditions was 40–50%. For luciferase assay, cells were simultaneously cotransfected with Renilla luciferase plasmid pRL-TK (50:1 mix of luciferase constructs and pRL-TK), harvested after 2 d using passive lysis buffer as described by the manufacturer (Promega, Madison, WI), and data are represented after normalization with Renilla luciferase. For immunofluorescence assay, cells after transfection and growth for 24 h were fixed in 2% paraformalde-hyde and stained with anti-β catenin antibodies or anti-AR (data not shown). Nuclear staining in these cells was detected by counterstaining with DAPI.

Image analysis

Oil Red O staining was quantified by image analysis using the Image Pro 4.01 software (Media Cybernetics, Silver Spring, MD), coupled to a Leica DMLB microscope/VCC video camera. After images were calibrated for background lighting, integrated OD (IOD = area $\times$ average intensity) was calculated using at least 20 pictures per treatment group (21). Results are proportional to the unweighted average OD, which was used to determine the Oil Red O staining retained in the fat cells. The experiment was repeated three times.

Statistics

Data are presented as mean $\pm$ sem. Differences between the groups were analyzed by ANOVA. If overall ANOVA revealed significant differences, then pairwise comparisons between groups were performed using Tukey's posttest procedure (see Figs. 2 and 6B) or Student's t test (see Figs. 3F, 6C, and 7B). All comparisons were two-tailed, and P values < 0.05 were considered statistically significant. The experiments were repeated three times, and data from representative experiments are shown.

Results

Expression of AR protein and mRNA in 3T3-L1 cells

Because no previous reports have investigated the expression of AR in 3T3-L1 cells, we used immunofluorescence and Western blot analysis to determine whether these cells express AR protein. Under basal conditions, AR immunofluorescence was detected mostly in the cytoplasm. In contrast, after DHT and testosterone treatment, most of the AR expression was detected in the nucleus (Fig. 1A). Western blot analysis confirmed that AR protein is expressed in untreated cells, and the AR protein expression levels remained unchanged after testosterone treatment (Fig. 1B). The AR mRNA expression was also

detected by real-time RT-PCR in this cell line (data not shown). Thus, our data demonstrate the expression of AR mRNA and protein in this preadipocyte cell line.

Effects of testosterone and DHT on adipogenic differentiation in 3T3-L1 cells: blockade of these effects by flutamide

To determine the effects of androgens on adipogenic differentiation, we treated confluent 3T3-L1 cells with or without graded concentrations of testosterone (0–100 n$_M$) and DHT (0–10 n$_M$) for 12 d. Differentiated 3T3-L1 cells in six-well plates after various treatments were stained with Oil Red O (representative pictures are shown in Fig. 2, *top*). We observed a dose-dependent reduction in the number of adipocytes after androgen treatment in a dose-dependent manner (Fig. 2, *top*); however, small changes in the overall sizes of adipocytes after androgen treatment cannot be ruled out. We further performed quantitative spectrophotometric analysis (OD, 520 nm) of Oil Red O-stained cells eluted with isopropanol, which revealed that testosterone and DHT both significantly inhibited adipogenic differentiation of these cells in a dose-dependent manner compared with the cells allowed to differentiate in control wells (Fig. 2, *bottom*). We observed that 100 n$_M$ testosterone caused $52 \pm 6\%$ inhibition, whereas 30 n$_M$ DHT was able to inhibit the adipogenesis by $40 \pm 5\%$. Flutamide (200 n$_M$), an AR antagonist, significantly blocked the inhibitory effects of both testosterone and DHT on the adipogenic differentiation of 3T3-L1 cells. Theses data suggest that testosterone and DHT both inhibit adipogenic differentiation of 3T3-L1 cells via an AR-dependent pathway.

Time course of C/EBP-β and C/EBP-δ expression in differentiating 3T3-L1 cells and effect of testosterone on their expression

To determine the effects of testosterone on the expression of early markers of adipogenic differentiation, we performed time course experiments with 3T3-L1 cells undergoing differentiation either in presence or absence of testosterone (100 n$_M$) treatment. The expression of C/EBP-β was detectable as early as 2 h and significantly decreased after 96 h of adipogenic differentiation. Testosterone inhibited the C/EBP-β expression at early times (2 h); however, at later time points, this effect was not significant (Fig. 3A). On the other hand, we observed that C/EBP-δ was expressed at a relatively later time point compared with C/EBP-β (8 h compared with 2 h) and peaked at about 24 h, and its levels were barely detectable after 96 h. Testosterone significantly inhibited C/EBP-δ expression in these cells at 2–24 h.

Testosterone and DHT inhibit key adipogenic transcription factors C/EBP-α and PPAR-γ2 in 3T3-L1 cells

We determined the effects of graded concentrations of testosterone and DHT on the protein and mRNA expression pattern of key adipogenic transcription factors C/EBP-α and PPAR-γ by Western blot analysis and quantitative real-time RT-PCR. Incubation of 3T3-L1 cells with testosterone (0–100 n$_M$) and DHT (0–10 n$_M$) for 12 d significantly inhibited the expression of 54-kDa PPAR-γ (Fig. 3B) and 42- and 30-kDa C/EBP-α (Fig. 3D) proteins in a dose-dependent manner. Densitometric analysis (Fig. 3C) of the respective bands showed 51 and 42% inhibition of PPAR-γ with 100 n$_M$ testosterone and 10 n$_M$ DHT, respectively.

Similarly, we observed 77 and 49% inhibition of C/EBP-α (sum of total intensity of 42- and 30-kDa bands) after testosterone and DHT treatment (Fig. 3E). Treatment of 3T3-L1 cells for 12 d with 0–100 n$_M$ testosterone also down-regulated PPAR-γ2 and C/EBP-α mRNA expression (Fig. 3F), as measured by real-time RT-PCR. Figure 3E demonstrates that PPAR-γ2 mRNA was significantly down-regulated by testosterone treatment; maximal inhibition was observed at 100 n$_M$ testosterone (~60% inhibition). Testosterone also down-regulated C/EBP-α mRNA in a dose-dependent manner; maximal inhibition was observed at 100 n$_M$ testosterone (~74%).

Time course of nuclear translocation of β-catenin in 3T3-L1 cells by testosterone and DHT treatment

To elucidate the possible mechanisms involved during testosterone- and DHT-induced inhibition of adipogenic differentiation, we performed immunofluorescence experiments to study the localization of β-catenin in these cells after treating the cells with 10 n$_M$ DHT and 100 n$_M$ testosterone for 24 h. We analyzed the localization of β-catenin, a key protein that translocated to the nucleus during activation of Wnt signaling after these treatments. In cells treated with medium alone, β-catenin was localized mainly in the cytoplasm and the cytoskeleton. A fraction of β-catenin protein translocated to the nucleus after testosterone (100 n$_M$) and DHT (10 n$_M$) treatment for 24 h (Fig. 4A). Simultaneous treatment of the 3T3-L1 cells with 10-fold molar excess of AR antagonist bicalutamide blocked testosterone- and DHT-induced nuclear translocation of β-catenin (Fig. 4A), suggesting that AR plays an important role during this process of β-catenin nuclear translocation. Lithium chloride treatment of these cells for 24 h also resulted in the nuclear translocation of β-catenin as expected.

We also performed a time course analysis of β-catenin nuclear translocation using nuclear and cytoplasmic fractions obtained after testosterone (100 n$_M$) and DHT (10 n$_M$) treatments for various time points (0.5–24 h) in 3T3-L1 cells (Fig. 4B). β-Catenin immunoreactivity was detectable in the nuclear fraction as early as 1 h after testosterone and DHT treatment, and there was a concomitant decrease in β-catenin protein in the cytoplasmic fractions, consistent with our data from the immunofluorescence experiments described in Fig. 4A. Simultaneous treatment of these testosterone-treated cells with bicalutamide resulted in decreased immunoreactivity for β-catenin protein in the nuclear fraction (Fig. 4B, *bottom*) after 24 h. These data indicate that DHT and testosterone activate Wnt signaling by translocating β-catenin to the nucleus in this preadipocyte cell line.

The shuttling of APC protein between different subcellular components and its control vary between different cell types and states (43, 44). To investigate the possible role of APC during testosterone- and DHT-induced inhibition of adipogenesis, we performed immunofluorescence experiments to study the localization of APC before and after treatment of the cells with the androgens. APC was expressed mostly in the nucleus under basal conditions (Fig. 4C), and there was no colocalization of APC with β-catenin in the nucleus after testosterone treatment (data not shown). Nuclear localization of APC has also been demonstrated in certain cell lines under basal conditions (43, 45, 46).

Physical interaction between AR, β-catenin, and TCF4 in DHT-treated 3T3-L1 cells

Using double immunofluorescence, we observed that AR and *β*-catenin were colocalized in the nucleus in both testosterone-treated (100 n_M) and DHT-treated (10 n_M) cells after 24 h (Fig. 5A) as observed by merging the AR- and *β*-catenin-stained pictures (*yellow*). The respective positions of the nuclei were detected by counterstaining the cells with DAPI (*blue*). We also performed immunoprecipitation experiments to evaluate the interaction between AR, *β*-catenin, and TCF4 using cell lysates obtained from 3T3-L1 cells after DHT (0–30 n_M) treatment (Fig. 5B). Protein extracts were immunoprecipitated using anti-AR (Fig. 5B, *top*) or anti-TCF4 antibody (Fig. 5B, *bottom*), and immunoprecipitates were analyzed by immunoblotting with anti-*β*-catenin, anti-AR, or anti-TCF4 antibodies (Fig. 5B, *top*) or with anti-*β*-catenin and anti-TCF4 or anti-AR antibodies. Except for a minimal AR-TCF4 interaction, these interactions were not detected in untreated cells, suggesting that DHT treatment was necessary for these interactions and complex formation. These interactions were significantly inhibited in the presence of 10-fold molar excess of bicalutamide (100 n_M), an AR antagonist. A higher concentration of DHT (30 n_M) led to an enhancement of this complex formation (Fig. 5B). These immunoprecipitation studies are consistent with our findings from immunofluorescence studies and demonstrate the translocation of *β*-catenin to the nucleus in a complex with AR and TCF4. Bicalutamide (100 n_M), an AR antagonist, blocked the DHT induction of *β*-catenin nuclear translocation. These data thus provide evidence of both *β*-catenin-AR and *β*-catenin-TCF4 interactions.

Testosterone's effects on adipogenic differentiation are blocked by Dn-TCF4 overexpression in 3T3-L1 cells

To investigate the role of TCF4-mediated pathways during testosterone's action on adipogenic differentiation, we over-expressed both full-lengthTCF4 and Dn-TCF4 in 3T3-L1 cells and tested the ability of testosterone to inhibit adipogenic differentiation under these conditions. We reasoned that if testosterone-induced AR and *β*-catenin interaction activates downstream Wnt signaling through TCF4, then overexpression of full-length TCF4 should directly inhibit fat cell formation; similarly, overexpression of Dn-TCF4 cDNA construct would be expected to block testosterone's inhibitory effects on adipogenic differentiation.

As expected, in 3T3-L1 cells, overexpressing TCF4 cDNA expression construct was associated with a significant inhibition of fat cell formation, as analyzed by Oil Red O staining of the fat cells (Fig. 6A). Testosterone treatment of 3T3-L1 cells that had been transfected with the TCF4 cDNA construct had no additional inhibitory effect on fat cell formation or adipogenic differentiation of 3T3-L1 cells, as measured by quantitative image analysis of the Oil Red O-positive cells (Fig. 6B). In contrast, 3T3-L1 cells transfected with Dn-TCF4 cDNA construct had a significantly greater number of adipocytes than control wells. Testosterone's inhibitory effects on preadipocyte differentiation were blocked by overexpresion of Dn-TCF4 cDNA construct (Fig. 6B), suggesting that TCF4 signaling pathway was necessary for mediating testosterone-induced inhibition of adipogenesis. Overexpression of TCF4 protein in these transfected cells was verified by Western blotting (data not shown).

To examine adipose gene regulation downstream from TCF4, we measured expression of mRNA in 3T3-L1 cells transfected with TCF4 or Dn-TCF4, by using real-time quantitative RT-PCR for the key adipogenic early marker C/EBP-α and late marker AP2 normalized to GAPDH (Fig. 6C). Overexpression of TCF4 in these preadipocytes significantly inhibited expression of C/EBP-α by over 50% and blocked AP2 by about 80% (Fig. 6C). However, Dn-TCF4 induced expression of both C/EBP-α by 50% and AP2 by 100% and prevented inhibition by testosterone (Fig. 6C). As a standard control, treatment of 3T3-L1 cells grown in AM with 20 m$_M$ LiCl, which activates Wnt signaling, resulted in almost complete inhibition of adipogenesis and also blocked expression of C/EBP-α and AP2 mRNA, as measured by quantitative RT-PCR (data not shown). Taken together, these data suggest that activation of downstream Wnt signaling pathway via AR/β-catenin/TCF4 plays an important role in mediating testosterone's inhibitory effects on adipogenic differentiation.

Testosterone up-regulation of Wnt target genes

Because androgen treatment induced AR interaction with β-catenin and androgen-induced nuclear translocation of β-catenin bypassed the canonical Wnt signaling for activation of TCF/LEF, we tested the ability of androgens to activate expression of some well-known downstream Wnt target genes including Lef1 and Fst. We performed SuperArray analysis of 3T3-L1 cells undergoing adipogenic differentiation either in the presence or absence of testosterone (100 n$_M$), using a Wnt gene-specific array. We observed that testosterone treatment led to significant activation of CD44 antigen, Fst, and Lef1 genes (Fig. 7A and Table 1).

We confirmed these findings by performing real-time quantitative RT-PCR analysis of mRNA expression using gene-specific primers (Fig. 7B). These data confirm that although testosterone did not induce canonical Wnt signaling, it activated AR/β-catenin interaction, their nuclear translocation, and activation of TCF4/LEF to activate known downstream Wnt-pathway target genes.

Constitutive activation of AR in 3T3-L1 cells does not inhibit adipogenic differentiation

To determine whether constitutively active AR protein fused with artificial coactivator VP16 inhibits adipogenesis in the absence of androgens, we expressed pACT- full-length AR (AR-VP16) and pARE$_4$-Luc and allowed the cells to differentiate in AM for 9 d. Cells were lysed, and C/EBP-α protein and mRNA levels were analyzed by Western blot and real-time RT-PCR analysis. We were unable to detect any significant changes in C/EBP-α mRNA (*left*) or protein (*right*) expression (Fig. 8A). Our densitometric scan of C/EBP-α protein (sum of 42- and 30-kDa) bands did not show a substantial change after normalization with GAPDH in samples where pAct-AR was expressed (data not shown). As a positive control to verify expression of activated AR-VP16 protein, plasmids encoding either pGL3 or pARE$_4$-Luc alone or AR-VP16 in combination with pARE$_4$-Luc along with pRLTK-Luc were transfected and changed to AM for another 48 h. The transfection efficiency under the conditions varied from 45–55%. The values were expressed after normalization with Renilla luciferase. We observed that luciferase activity was significantly higher (~75 ± 6-fold) in cells cotransfected with both AR-VP16 and pARE$_4$-Luc compared with individual vectors alone (Fig. 8B), providing evidence that AR is constitutively active. We also analyzed the

subcellular localization of AR (data not shown) and β-catenin in these cells in which AR was constitutively active; we were unable to detect any nuclear translocation of β-catenin under these condition (Fig. 8C). To measure expression of an endogenous AR-responsive gene, we further analyzed the expression of p21 protein after transfection. We observed that p21 level was significantly induced in cells transfected with pAct-AR compared with pARE$_4$-Luc vector (Fig. 8D), suggesting that constitutively activated AR is able to activate endogenous AR-responsive genes.

Discussion

The data presented in this manuscript constitute the first demonstration that testosterone's inhibitory effects on preadipocyte differentiation are transduced through AR-mediated activation of a noncanonical Wnt/β-catenin signaling that activates downstream TCF/LEF factors while bypassing several proximal steps in the canonical Wnt pathway. Testosterone and DHT inhibited the differentiation of 3T3-L1 preadipocytes into mature adipocytes and down-regulated the mRNA and protein expression of key adipogenic transcription factors, C/EBP-δ, C/EBP-α, and PPAR-γ2, in a time- and concentration-dependent manner. These antiadipogenic effects of testosterone and DHT were blocked by an AR antagonist, flutamide, indicating that these effects were transduced through an AR-mediated pathway, supported by the fact that AR mRNA and protein were expressed in these cells. Both testosterone and DHT induced AR translocation and colocalization with β-catenin in the nucleus within 1 h of treatment. The AR protein formed a molecular complex with β-catenin and TCF4, and this interaction was androgen dependent because it was blocked when cells were treated simultaneously with 10-fold molar excess of a specific AR antagonist, bicalutamide. Androgen inhibition of fat cell differentiation and C/EBP-α and AP2 mRNA expression was mimicked by TCF4 overexpression but blocked by Dn-TCF4 in 3T3-L1 cells. These data lead us to conclude that androgens inhibit adipogenic differentiation of 3T3-L1 preadipocytes by activating noncanonical Wnt through activation of AR/β-catenin-TCF4.

During early adipogenesis, a cascade of transcription factors is sequentially induced, including C/EBP-β and C/EBP-δ at early time points, followed by C/EBP-α and PPAR-γ2 (47). The expression of C/EBP-β and C/EBP-δ was induced within 2–24 h in 3T3-L1 cells grown in AM for various times. Treatment with testosterone significantly inhibited expression levels of C/EBP-δ and subsequently C/EBP-α and PPAR-γ2.

In a series of elegant studies, McDougald and colleagues (35, 36) have demonstrated that the Wnt signaling pathway plays an important role in regulation of adipogenic differentiation; however, the regulation of Wnt signaling pathway by androgens during adipogenic differentiation has not been previously studied. Wnts, a group of soluble secretory proteins, are important molecular switches that govern adipo-genesis by inhibiting C/EBP-α and PPAR-γ2 (35, 36, 38, 41). Disruption of extracellular Wnt signaling by soluble Wnt inhibitors, soluble frizzled receptor proteins-1 and –2 (36) or by overexpression of a Dn-TCF4 construct results in up-regulation of C/EBP-α and PPAR-γ2 and spontaneous adipogenesis (35, 47). Our data provide direct evidence of the androgen-dependent interaction of AR and β-catenin in 3T3-L1 preadipocytes. Using double

immunofluorescence, we demonstrated the colocalization of AR and β-catenin in the nucleus in a ligand-dependent manner. The immuno-precipitation studies provided additional confirmation of the physical interaction between AR and β-catenin and between β-catenin and TCF4; these interactions were androgen dependent and were significantly inhibited in the presence of the AR antagonist bicalutamide.

The most compelling evidence for the involvement of an AR/β-catenin/TCF4 pathway in mediating androgen inhibition of adipogenic differentiation emerged from our experiments that used Dn-TCF4 cDNA constructs. In 3T3-L1 preadipocytes, transfection with Dn-TCF4 cDNA construct not only increased adipogenesis but also blocked testosterone's effects on adipogenic differentiation. Thus, disruption of TCF4 and the consequent inhibition of downstream Wnt signaling resulted in an induction in overall adipogenic differentiation as expected and attenuation of testosterone's effects on adipogenesis. Conversely, when TCF4 was constitutively overexpressed using a cDNA construct, adipo-genesis was inhibited, and concomitant incubation with testosterone had no additional effect on adipogenesis. Although this does not prove that the TCF4 factor, as opposed to LEF1, is the endogenous molecule that mediates the androgen effect, it shows that this downstream Wnt signaling pathway is involved during the process. These results were confirmed in other experiments in which we used nucleofection of these constructs in 3T3-L1 cells and achieved over 70% transfection efficiency. Taken together, these data point to the pivotal role of a functional AR/β-catenin/ TCF4 pathway in mediating androgen effects on modulating adipogenesis.

Our studies provide additional evidence of the cross-communication between AR-mediated intracellular signaling and the downstream Wnt signal transduction cascade. Addition of androgen to the incubation medium was associated with AR translocation into the nucleus and its association with β-catenin, as confirmed by double-immunofluorescence studies. This interaction was ligand dependent and blocked by an AR antagonist. The immunoprecipitation experiments provided additional proof of the physical interaction between AR and β-catenin in the nuclear fraction of 3T3-L1 cells. Our data are thus consistent with previous reports that AR promotes nuclear translocation of β-catenin in prostate cancer and other cells through specific protein-protein interaction in a ligand-dependent manner (23–26). A strong interaction between the ligand binding domain of AR and the first six armadillo repeats of β-catenin has been demonstrated (23, 24). β-Catenin has been shown to interact with AR but not with other steroid hormone receptors.

During canonical Wnt signaling, β-catenin is translocated to the nucleus in association with APC protein, which remains in the cytoplasm under normal conditions and is trans-located to the nucleus after Wnt activation along with β-catenin, to activate Wnt target genes through the TCF4-mediated pathway. However, in our experiments, nuclear translocation of β-catenin was independent of APC. APC immunofluorescence was predominantly localized in the nucleus, and we were unable to detect colocalization of β-catenin and APC either by double immunofluorescence or by immuno-precipitation either under basal conditions or after androgen treatment. Similar nuclear localization of APC has been reported in several other cells under basal conditions (44–46).

The data reported in this manuscript provide evidence that androgens inhibit differentiation of preadipocytes into mature adipocytes; these data are consistent with previous reports that testosterone inhibits fat cell differentiation of adipocyte precursor cells (10–12, 17). However, these studies do not exclude the possibility that androgens might exert additional effects at other steps in the adipogenic process. Our demonstration of androgen suppression of preadipocyte differentiation is only one possible mechanism of fat mass inhibition. In fact, previous reports suggest that testosterone may modulate body composition by exerting additional effects on lipid metabolism in fully differentiated fat cells (12). We have demonstrated previously that testosterone and DHT promote myogenic commitment and/or differentiation and inhibit adipogenic differentiation and PPAR-γ2 and C/EBP-α expression in mesenchymal C3H 10T1/2 pluripo-tent cells (21). Testosterone also has been reported to suppress lipid uptake and LPL activity in adipocytes (12). Dieudonne *et al.* (11) reported that testosterone and DHT inhibit GAPDH activity significantly in epididymal preadipocytes. The net result of these androgen actions at multiple sites in the adipogenic and lipogenic processes is a reduction in fat mass.

Our findings have clinical relevance because they provide a rational mechanistic explanation for the observed decrease in whole-body fat mass during testosterone supplementation in human studies. We understand that our current findings using 3T3-L1 cells as a model system is not an accurate measure of what occurs in human preadipocytes. However, it still has important implications for drug discovery, especially development of selective AR modulators. Testosterone and DHT inhibit preadipocyte differentiation by activation of downstream target genes through noncanonical Wnt signaling. The intracellular events triggered by androgen binding to the AR are cross-communicated to the Wnt signaling pathway through an association of AR with β-catenin and translocation of this complex to the cell nucleus. This results in downstream activation of TCF4/LEF and inhibition of adipogenesis, involving suppression of key adipogenic factors PPAR-γ2, C/EBP-δ, and C/EBP-α and also activation of several Wnt pathway target genes including Fst, Lef1, and CD44 antigen (48–50). We also tested whether constitutively active AR fused with artificial coactivator VP16 (51, 52) is sufficient to inhibit adipogenesis in the absence of androgen and nuclear β-catenin. We observed that constitutive AR activation alone in these cells does not inhibit C/EBP-α mRNA and protein expression or β-catenin translocation, although it significantly induced the protein expression of p21, an AR-responsive gene containing ARE in the promoter region (22). These findings might suggest that inhibition of adipogenesis in 3T3-L1 cells by androgens is mediated preferably through TCF4/LEF sites. Additional work is in progress to investigate this important aspect of androgen regulation of adipogenesis in details. The molecular events that follow TCF4 activation and result in inhibition of adipogenic differentiation are not well understood and need future investigation.

Acknowledgments

Abbreviations

AM	Adipogenic medium
AP2	fatty acid binding protein 2
APC	adenomatous polyposis coli
AR	androgen receptor
ARE	androgen response element
C/EBP	CCAAT/enhancer binding protein
DHT	dihydrotestosterone
Dn	dominant negative
FBS	fetal bovine serum
FITC	fluorescein isothiocyanate
Fst	follistatin
GAPDH	glyceraldehyde-3-phosphate dehydrogenase
GM	growth medium
LEF	lymphoid-enhancer factor
LPL	lipoprotein lipase
PPAR	peroxisome proliferator-activated receptor
TCF	T-cell factor

References

1. Mauras N, Hayes V, Welch S, Rini A, Helgeson K, Dokler M, Veldhuis JD, Urban RJ. Testosterone deficiency in young men: marked alterations in whole body protein kinetics, strength, and adiposity. J Clin Endocrinol Metab. 1998; 83:1886–1892. [PubMed 9626114]

2. Matsumoto T, Takeyama K, Sato T, Kato S. Androgen receptor functions from reverse genetic models. J Steroid Biochem Mol Biol. 2003; 85:95–99. [PubMed: 12943692]

3. Wilson JD. Androgen abuse by athletes. Endocr Rev. 1988; 9:181–191. [PubMed: 3042375]

4. Bhasin S, Woodhouse L, Casaburi R, Singh AB, Bhasin D, Berman N, Chen X, Yarasheski KE, Magliano L, Dzekov C, Dzekov J, Bross R, Phillips J, Sinha-Hikim I, Shen R, Storer TW. Testosterone dose-response relationships in healthy young men. Am J Physiol Endocrinol Metab. 2001; 281:E1172–E1181. [PubMed: 11701431]

5. Snyder PJ, Peachey H, Berlin JA, Hannoush P, Haddad G, Dlewati A, Santanna J, Loh L, Lenrow DA, Holmes JH, Kapoor S, Atkinson L, Strom S. Effects of testosterone replacement in hypogonadal men. J Clin Endocrinol Metab. 2000; 85:2670–2677. [PubMed: 10946864]

6. Bhasin S, Storer TW, Berman N, Yarasheski KE, Clevenger B, Phillips J, Lee WP, Bunnell TJ, Casaburi R. Testosterone replacement increases fat-free mass and muscle size in hypogonadal men. J Clin Endocrinol Metab. 1997; 82:407–413. [PubMed: 9024227]

7. Snyder PJ, Peachey H, Hannoush P, Berlin JA, Loh L Lenrow DA, Holmes JH, Dlewati A, Santanna J, Rosen CJ, Strom BL. Effect of testosterone treatment on body composition and muscle

strength in men over 65 years of age. J Clin Endocrinol Metab. 1999; 84:2647–2653. [PubMed: 10443654]

8. Bhasin S, Storer TW, Javanbakht M, Berman N, Yarasheski KE, Phillips J, Dike M, Sinha-Hikim I, Shen R, Hays RD, Beall G. Testosterone replacement and resistance exercise in HIV-infected men with weight loss and low testosterone levels. JAMA. 2000; 283:763–778. [PubMed: 10683055]

9. Grinspoon S, Corcoran C, Askari H, Schoenfeld D, Wolf L, Burrows B, Walsh M, Hayden D, Parlman K, Anderson E, Basgoz N, Klibanski A. Effects of androgen administration in men with the AIDS wasting syndrome. A randomized, double blind, placebo-controlled trial. Ann Intern Med. 1998; 129:18–26. [PubMed: 9652995]

10. Garcia E, Lacasa M, Agli B, Giudicelli Y, Lacasa D. Modulation of rat preadipocyte adipose conversion by androgenic status: involvement of C/EBPs transcription factors. J Endocrinol. 1999; 161:89–97. [PubMed: 10194532]

11. Dieudonne MN, Pecquery R, Leneveu MC, Giudicelli Y. Opposite effects of androgens and estrogens on adipogenesis in rat preadipocytes: evidence for sex and site-related specificities and possible involvement of insulin-like growth factor 1 receptor and peroxisome proliferator-activated receptor-γ2. Endocrinology. 2000; 141:649–656. [PubMed: 10650946]

12. Ramirez ME, McMurry MP, Wiebke GA, Felten KJ, Ren K, Meikle AW, Iverius PH. Evidence for sex steroid inhibition of lipoprotein lipase in men: comparison of abdominal and femoral adipose tissue. Metabolism. 1997; 46:179–185. [PubMed: 9030826]

13. Brodsky IG, Balagopal P, Nair KS. Effects of testosterone replacement on muscle mass and muscle protein synthesis in hypogonadal men: a clinical research center study. J Clin Endocrinol Metab. 1996; 81:3469–3475. [PubMed: 8855787]

14. Marin P, Holmang S, Jonsson L, Sjostrom L, Kvist H, Holm G, Lindstedt G, Bjorntorp P. The effects of testosterone treatment on body composition and metabolism in middle-aged obese men. Int J Obes Relat Metab Disord. 1992; 16:991–997. [PubMed: 1335979]

15. Marin P, Oden B, Bjorntorp P. Assimilation and mobilization of triglycerides in subcutaneous abdominal and femoral adipose tissue in vivo in men: effects of androgens. J Clin Endocrinol Metab. 1995; 80:239–243. [PubMed: 7829619]

16. Marin P, Krotkiewski M, Bjorntorp P. Androgen treatment of middle-aged, obese men: effects on metabolism, muscle and adipose tissues. Eur J Med. 1992; 1:329–336. [PubMed: 1341460]

17. Dieudonne MN, Pecquery R, Boumediene A, Lenevew MC, Giudicelli Y. Androgen receptors in human preadipocytes and adipocytes: regional specificities and regulation by sex steroids. Am J Physiol. 1998; 274:C1645–C1652. [PubMed: 9611130]

18. Jaubert AM, Pecquery R, Sichez L, Dieudonne MN, Cloix JF, Giudicelli Y. Androgen receptors in hamster white adipocytes and their precursor cells: regional variations and modulation by androgens. Endocrine. 1993; 1:535–540.

19. Mooradian AD, Morley JE, Korenman SG. Biological actions of androgens. Endocr Rev. 1987; 8:1–28. [PubMed: 3549275]

20. Mangelsdorf DJ, Thummel C, Beato M, Herrlich P, Schutz G, Umesono K, Blumberg B, Kastner P, Mark M, Chambon P, Evans RM. The nuclear receptor superfamily: the second decade. Cell. 1995; 83:835–839. [PubMed: 8521507]

21. Singh R, Artaza JN, Taylor WE, Gonzalez-Cadavid NF, Bhasin S. Androgens stimulate myogenic differentiation and inhibit adipogenesis in C3H 10T1/2 pluripotent cells through an androgen receptor-mediated pathway. Endocrinology. 2003; 44:5081–5088. [PubMed: 12960001]

22. Yeh S, Tsai M-Y, Xu Q, Mu XM, Lardy H, Huang KE, Lin H, Yeh SD, Altuwaijri S, Zhou X, Xing L, Boyce BF, Hung MC, Zhang S, Gan L, Chang C, Hung MC. Generation and characterization of androgen receptor knockout (ARKO) mice: an in vivo model for the study of androgen functions in selective tissues. Proc Natl Acad Sci USA. 2002; 99:13498–13503. [PubMed: 12370412]

23. Mulholland DJ, Cheng H, Reid K, Rennie PS, Nelson CC. The androgen receptor can promote β-catenin nuclear translocation independently of adenomatous polyposis coli. J Biol Chem. 2002; 277:17933–17943. [PubMed: 11856748]

24. Pawlowski JE, Ertel JR, Allen MP, Xu M, Butler C, Wilson EM, Wierman ME. Liganded androgen receptor interaction with β-catenin: nuclear co-localization and modulation of

transcriptional activity in neuronal cells. J Biol Chem. 2002; 277:20702–20710. [PubMed: 11916967]

25. Yang F, Li X, Sharma M, Sasaki CY, Longo DL, Lim B, Sun Z. Linking β-catenin to androgen-signaling pathway. J Biol Chem. 2002; 277:11336–11344. [PubMed: 11792709]

26. Truica CI, Byers S, Gelmann EP. β-Catenin affects androgen receptor transcriptional activity and ligand specificity. Cancer Res. 2000; 60:4709–4713. [PubMed: 10987273]

27. Cadigan KM, Nusse R. Wnt signaling: a common theme in animal development. Genes Dev. 1997; 11:3286–3305. [PubMed: 9407023]

28. Cossu G, Borello U. Wnt signaling and the activation of myogenesis in mammals. EMBO J. 1999; 24:6867–6872. [PubMed: 10601008]

29. Nelson WJ, Nusse R. Convergence of Wnt, β-catenin, and cadherin pathways. Science. 2004; 303:1483–1487. [PubMed: 15001769]

30. Yanfeng W, Saint-Jeannet JP, Klein PS. Wnt-frizzled signaling in the induction and differentiation of the neural crest. Bioessays. 2003; 25:317–325. [PubMed: 12655639]

31. Kawano Y, Kypta R. Secreted antagonists of the Wnt signalling pathway. J Cell Sci. 2003; 116:2627–2634. [PubMed: 12775774]

32. Polakis P. Wnt signaling and cancer. Genes Dev. 2000; 14:1837–1851. [PubMed: 10921899]

33. Morin PJ. β-Catenin signaling and cancer. Bioessays. 1999; 21:1021–1030. [PubMed: 10580987]

34. Longo KA, Wright WS, Kang S, Gerin I, Chiang SH, Lucas PC, Opp MR, MacDougald OA. Wnt10b inhibits development of white and brown adipose tissues. J Biol Chem. 2004; 279:35503–35509. [PubMed: 15190075]

35. Ross SE, Hemati N, Longo KA, Bebbett CN, Jucas PC, Erickson RL, Mac-Dougald OA. Inhibition of adipogenesis by Wnt signaling. Science. 2000; 289:950–953. [PubMed: 10937998]

36. Bennet CN, Ross SE, Longo KA, Bajnok L, Hemati N, Johnson KW, Harrison SD, MacDougald OA. Regulation of Wnt signaling during adipogenesis. J Biol Chem. 2002; 277:30998–31004. [PubMed: 12055200]

37. Gregoire FM, Smas CA, Sul HS. Understanding adipocyte differentiation. Physiol Rev. 1998; 78:783–808. [PubMed: 9674695]

38. Rosen ED, Hsu C-H, Wang X, Sakai S, Freeman MW, Gonzalez FJ, Spigelman BM. C/EBP-α induces adipogenesis through PPARγ: a unified pathway. Genes Dev. 2002; 16:22–26. [PubMed: 11782441]

39. Green H, Kehinde O. Spontaneous heritable changes leading to increased adipose conversion in 3T3 cells. Cell. 1976; 1:105–113. [PubMed: 949738]

40. Lu S, Liu M, Epner DE, Tsai SY, Tsai MJ. Androgen regulation of the cyclin-dependent kinase inhibitor p21 gene through an androgen response element in the proximal promoter. Mol Endocrinol. 1999; 13:376–384. [PubMed: 10076995]

41. Hemati N, Ross SE, Erickson RL, Groblewski GE, MacDougald OA. Signaling pathways through which insulin regulates CCAAT/enhancer binding protein-α (C/EBP-α) phosphorylation and gene expression in 3T3–L1 adipocytes. Correlation with GLUT4 gene expression. J Biol Chem. 1997; 272:25913–25919. [PubMed: 9325324]

42. Artaza JN, Bhasin S, Mallidis C, Taylor W, Ma K, Gonzalez-Cadavid NF. Endogenous expression and localization of myostatin and its relation to myosin heavy chain distribution in C2C12 skeletal muscle cells. J Cell Physiol. 2002; 190:170–179. [PubMed: 11807821]

43. Bienz M. The subcellular destinations of APC proteins. Nat Rev Mol Cell Biol. 2002; 3:328–338. [PubMed: 11988767]

44. Fearnhead NS, Britton MP, Bodmer WF. The ABC of APC. Hum Mol Genet. 2001; 10:721–733. [PubMed: 11257105]

45. Neufeld KL, White RL. Nuclear and cytoplasmic localization of adenomatous polyposis coli protein. Proc Natl Acad Sci USA. 1997; 94:3034–3039. [PubMed: 9096341]

46. Zhang F, White RL, Neufeld KL. Cell density and phosphorylation control the subcellular localization of adenomatous polyposis coli protein. Mol Cell Biol. 2001; 21:8143–8156. [PubMed: 11689703]

47. MacDougald OA, Lane MD. Transcriptional regulation of gene expression during adipocyte differentiation. Annu Rev Biochem. 1995; 64:345–373. [PubMed: 7574486]

48. Hovanes K, Li TW, Munguia JE, Truong T, Milovanovic T, Lawrence Marsh J, Holcombe RF, Waterman ML. β-Catenin-sensitive isoforms of lymphoid enhancer factor-1 are selectively expressed in colon cancer. Nat Genet. 2001; 28:53–57. [PubMed: 11326276]

49. Willert J, Epping M, Pollack JR, Brown PO, Nusse R. A transcriptional response to Wnt protein in human embryonic carcinoma cells. BMC Dev Biol. 2002; 2:8. [PubMed: 12095419]

50. Wielenga VJ, Smits R, Korinek V, Smit L, Kielman M, Fodde R, Clevers H, Pals ST. Expression of CD44 in Apc and Tcf mutant mice implies regulation by the WNT pathway. Am J Pathol. 1999; 154:515–523. [PubMed: 10027409]

51. Sui X, Bramlett KS, Jorge MC, Swanson DA, von Eschenbach AC, Jenster G. Specific androgen receptor activation by an artificial coactivator. J Biol Chem. 1999; 274:9449–9454. [PubMed: 10092626]

52. Yuan X, Lu ML, Li T, Balk SP. SRY interacts with and negatively regulates androgen receptor transcriptional activity. J Biol Chem. 2001; 276:46647–46654. [PubMed: 11585838]
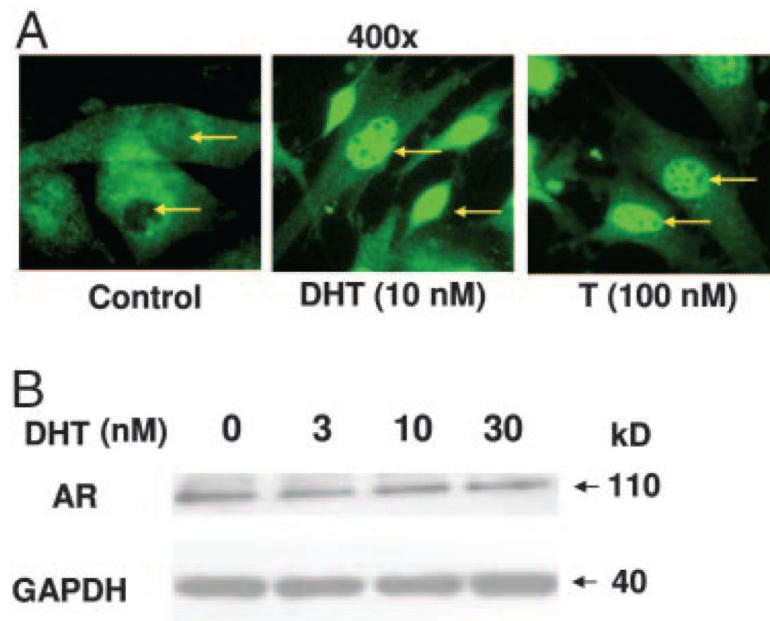
Fig. 1.
AR expression in 3T3-L1 cells. A, Immunocytochemical detection: 3T3-L1 preadipocytes were plated on 8-well chamber slides, either in the presence or the absence of DHT (10 n_M) or T (100 n_M) for 24 h. The cells were fixed with 2% paraformaldehyde and AR protein was detected by immunofluorescence using a polyclonal anti-AR antibody and FITC-conjugated secondary antibody (*green*). The *arrows* show the location of nuclei. B, Western blot analysis: Cells were treated with various concentrations of DHT (0–30 n_M) for 24 h, harvested, and analyzed by Western blot analysis using anti-AR antibody. The membrane was stripped and reprobed with anti-GAPDH antibody.
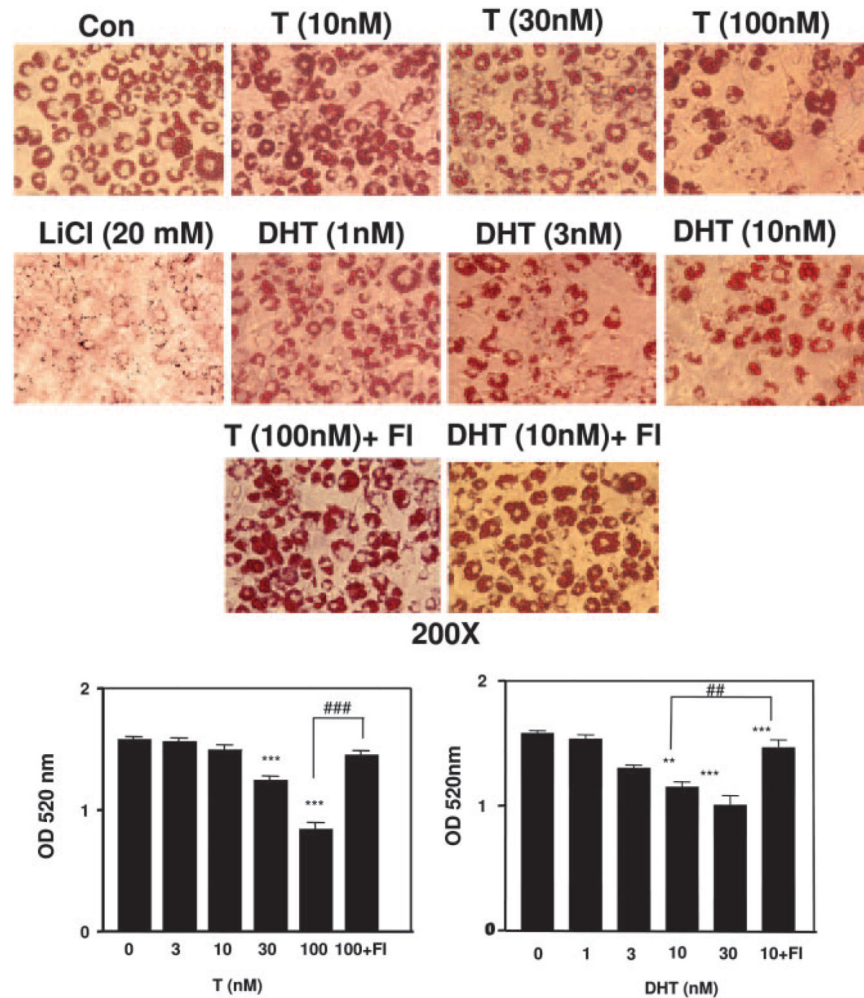
Fig. 2.

Testosterone and DHT inhibit adipogenic differentiation of 3T3-L1 preadipocytes. *Top panel*, 3T3-L1 cells were induced to differentiate in 6-well plates for 12 d as described in *Materials and Methods* with various concentrations of testosterone (T) and DHT. In certain conditions, cells were simultaneously treated with flutamide (Fl is 200 nM flutamide). Cells were fixed with 2% paraformaldehyde and stained with 0.5% Oil Red O stain. Representative photomicrographs (200×) are shown for each treatment group. *Bottom panel*, 3T3-L1 (4×10^5) preadipocytes were induced to differentiate for 12 d with or without various treatments (androgens and 200 nM flut-amide), fixed with 2% paraformaldehyde, and stained with 0.5% Oil Red O. Quantitative analysis of adipocyte differentiation was done by measuring the OD 520 nm of the Oil Red O-stained adipocytes eluted with isopropanol and Igepal CA 40. The data represent the mean ± SEM of three independent experiments (significance: **, $P < 0.01$; ***, $P < 0.001$ compared with control group; and ##, $P < 0.01$; and ###, $P < 0.001$ compared with DHT (10) and T (100) groups, respectively).
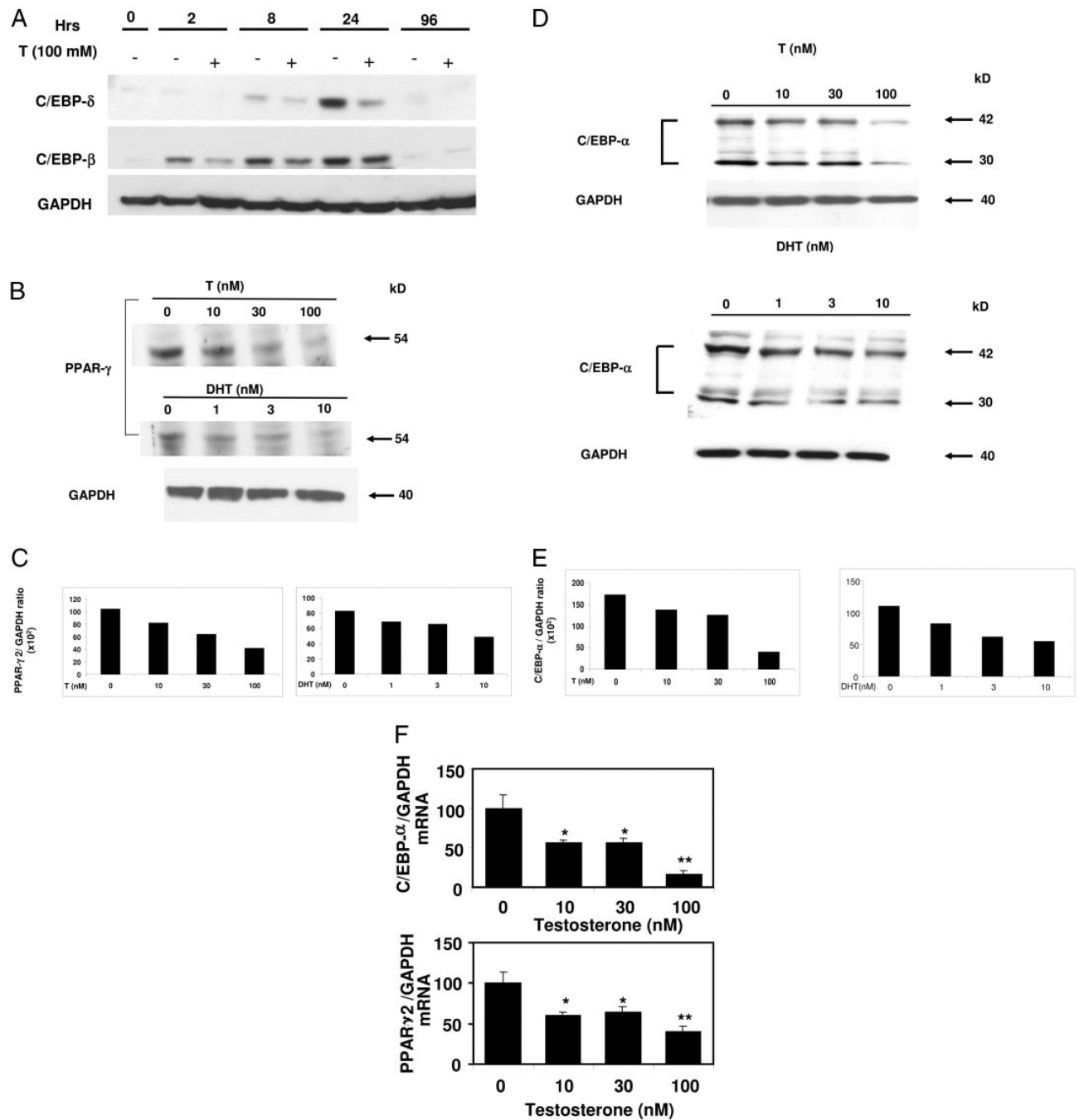
Fig. 3.
Time course of C/EBP-β and C/EBP-δ expression during adipogenic differentiation with and without androgens and dose-dependent inhibition of C/EBP-α and PPAR-γ expression in 3T3-L1 preadipocytes by androgens. A, Confluent 3T3-L1 cells were treated with 100 n$_M$ testosterone (T) and allowed to differentiate in AM for various time points. Cells were harvested, lysed, and 100 μg of total protein was electrophoresed on SDS-containing polyacrylamide gels, and Western blot analysis was performed using anti-C/EBP-β, anti-C/EBP-δ, or anti-GAPDH antibodies. Three independent experiments were conducted and data

from one representative experiment are shown. B, *Top panel*, 3T3-L1 cells were treated with either testosterone (0–100 n$_M$) or DHT (0–10 n$_M$) for 12 d and allowed to differentiate in AM as described in *Materials and Methods*. Cells were harvested, lysed, and 100 μg of total protein was electrophoresed on SDS-containing polyacrylamide gels, and Western blot analysis was performed using anti-C/EBP-α, anti-PPAR-γ, or anti-GAPDH antibodies. Three independent experiments were conducted and data from one representative experiment are shown. C, Densitometric analysis of the PPAR-γ expression (B, *top panel*) in 3T3-L1 cells after various doses of androgens normalization with GAPDH. D, 3T3-L1 cells were treated with testosterone (0 –100 n$_M$) or DHT (0 –10 n$_M$) and allowed to differentiate in AM as in panel B for 12 d. Cells were harvested, lysed, and 100 μg of total protein was electrophoresed on SDS-containing polyacrylamide gels, and Western blot analysis was performed using anti-C/EBP-α or anti-GAPDH antibodies. Three independent experiments were conducted and data from one representative experiment are shown. E, Densitometric analysis of the expression of C/EBP-α protein (panel C) in 3T3-L1 cells with various doses of androgens after normalization with GAPDH. F, Total cellular RNA from 3T3-L1 cells was prepared using Trizol reagent after incubation with graded concentrations of testosterone (0–100 n$_M$) for 12 d. Quantitative analysis of C/EBP-α and PPAR-γ2 mRNA levels was performed by real-time RT-PCR after normalizing with GAPDH using gene-specific primers. (Significance: *, $P < 0.02$; and **, $P < 0.005$ compared with the control group.)
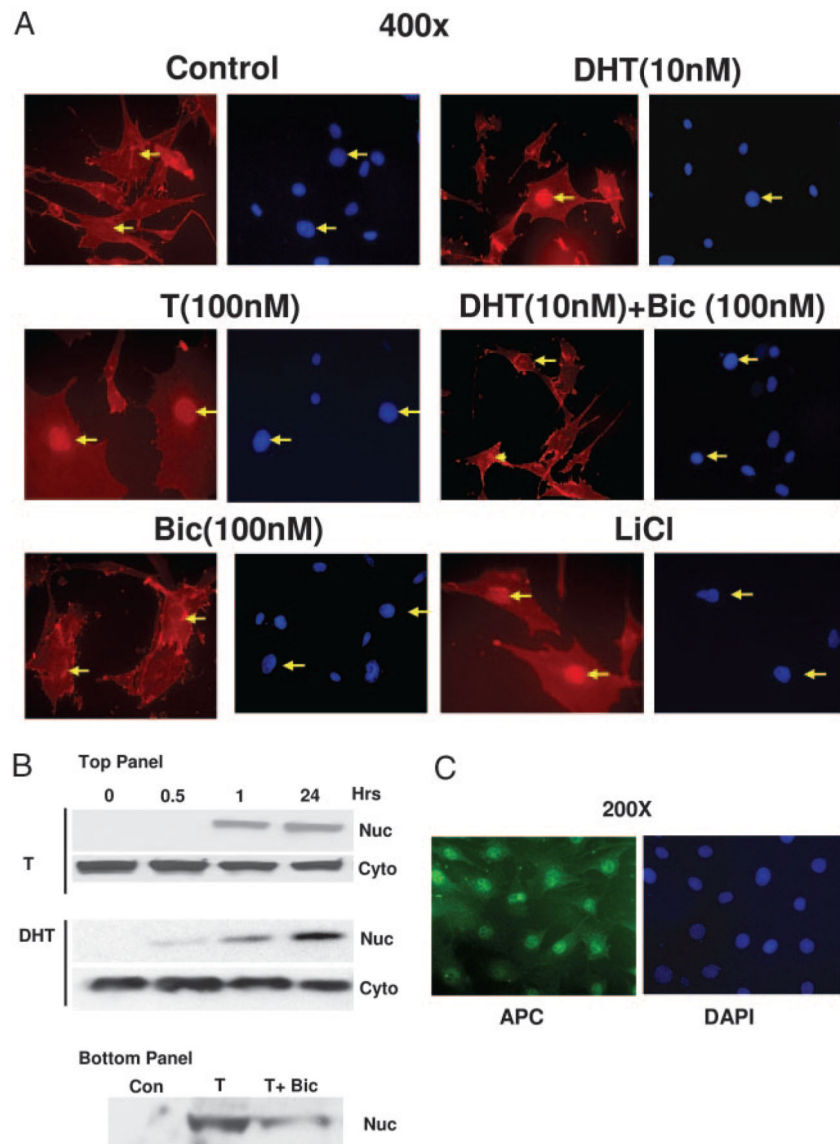
Fig. 4.
AR mediated nuclear translocation of β-catenin in 3T3-L1 preadipocyte cells after testosterone or DHT treatment. A, Cells were grown for 24 h on eight-well chamber slides at 40% confluence and fixed for 20 min with 2% paraformaldehyde after various treatments, as shown. Localization of β-catenin was detected by using anti-β-catenin antibody and Texas Red-conjugated secondary antibody (*red*). The cells were counter stained with a nuclear stain DAPI (*blue*). B, *Top panel*, Cells were treated with T (100 nM) or DHT (10 nM) for various time points (0–24 h) and nuclear and cytoplasmic fractions were analyzed by Western blot analysis using anti-β catenin antibody. *Bottom panel*, Cells grown with none (control), T (100 nM) or T+ Bic (300 nM bicalutamide) for 24 h, nuclear and cytoplasmic fractions were analyzed by Western blot analysis using anti-β catenin antibody. C, Cells were treated as described in panel A, and localization of APC was detected by using anti-APC antibody and FITC conjugated secondary antibody. The data for androgen treatment

groups are not shown. The *arrows* show the location of the nuclei. The cells were also counterstained with DAPI (*blue*).
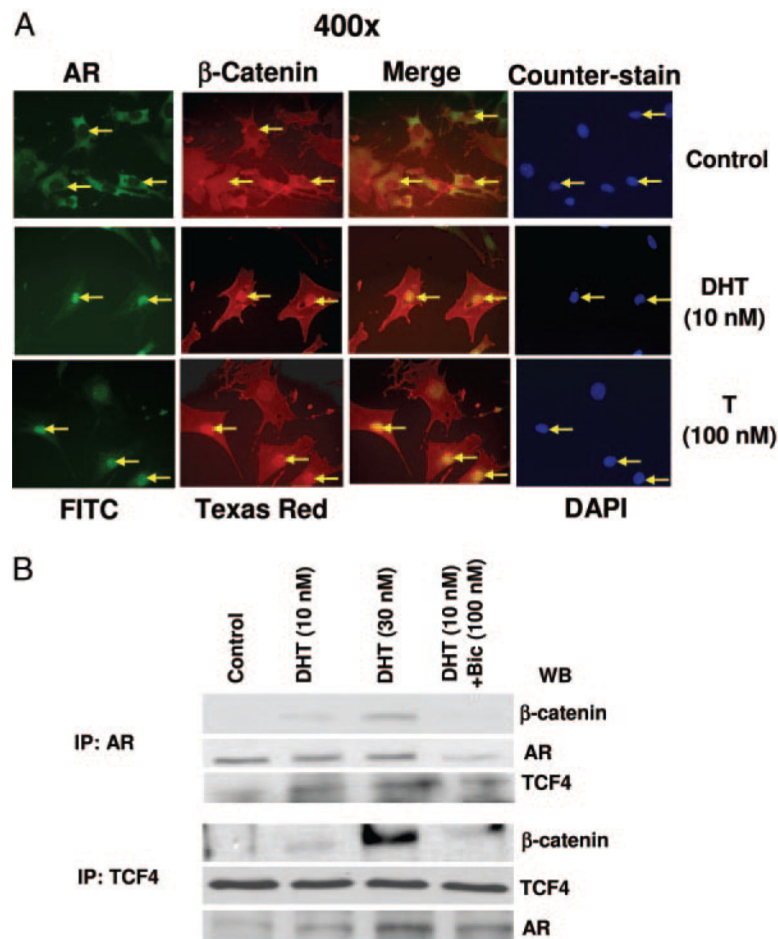
Fig. 5.
Colocalization and physical interaction of AR and TCF4 with *β*-catenin in DHT-treated
cells. A, Double immunofluorescence: Cells were treated as described in Fig. 4 and double
immunofluorescence experiments were performed using anti-AR and FITC-labeled
secondary antibody for the detection of AR (*green*) and Texas Red-conjugated secondary
antibody for the detection of *β*-catenin (*red*), and merging of the *red* and *green* pictures are
shown as *yellow*. Cells were counterstained with DAPI (*blue*) to localize the position of
nuclei in these cells. B, Immunoprecipitation: Cells were treated with either DHT (10 and 30
n$_M$) alone or with bicalutamide (100 n$_M$) for 24 h and immunoprecipitation was carried out
using 500 *μ*g of total cell lysates and 1–2 *μ*g of respective primary antibodies (see *Materials
and Methods*). The immunoprecipitated proteins were analyzed by Western blot analysis.
Upper panel shows the detection of *β*-catenin, AR, and TCF4 bands after
immunoprecipitation with anti-AR antibody, and *lower panel* shows the detection of *β*-
catenin and TCF4 bands after immunoprecipitation with anti-TCF4 antibody.
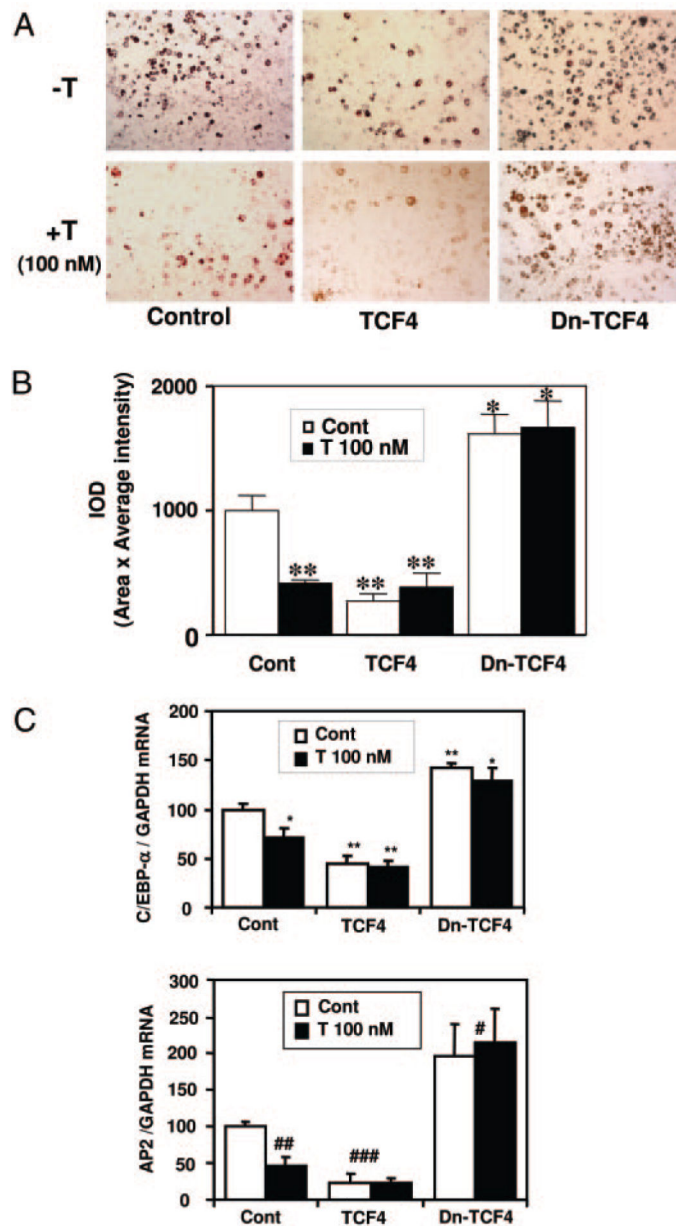
Fig. 6.
Inhibition of adipogenic differentiation in 3T3-L1 cells by testosterone is blocked by overexpression of TCF4 or a dominant negative TCF4 construct. 3T3-L1 cells were transfected either with full-length TCF4 or a dominant negative TCF4 (Dn-TCF4) cDNA construct or a control vector and were allowed to differentiate either in the presence (+T) or in the absence (−T) of testosterone (100 n_M) for 12 d. Cells were fixed and stained with Oil Red O and quantitative image analysis was performed. A, Oil Red O staining: Representative photographs of Oil Red O-stained adipocytes are shown from different treatment groups (panel A). B, The graph shows the quantitative image analysis data obtained after averaging 20 fields from each treatment group, mock (Cont), TCF4 transfection (TCF4), and Dn-TCF4 transfection (Dn-TCF4) (P values *vs.* control: *, P <

0.05; IOD denotes integrated optical density; T denotes testosterone). C, Real-time quantitative RT-PCR analysis demonstrating the effects of testosterone on C/EBP-α and AP2 mRNA expression in TCF4 and Dn-TCF4 overexpressed 3T3-L1 cells 3T3-L1 cells were transfected with full-length TCF4 or Dn-TCF4 or a control vector plasmid and were allowed to differentiate in adipogenic medium (3 d) then GM with or without testosterone (100 n$_M$) for 9 d as in panel A. Total cellular RNA was isolated and C/EBP-α and AP2 mRNA expression was analyzed by real-time RT-PCR. [*, $P < 0.03$ and **, $P < 0.0005$ denotes P values *vs.* control group (no T) in the *upper panel*; whereas #, $P < 0.05$, ##, $P < 0.01$ and ###, $P < 0.002$ denotes P values *vs.* control group (no T) in the *lower panel*.]
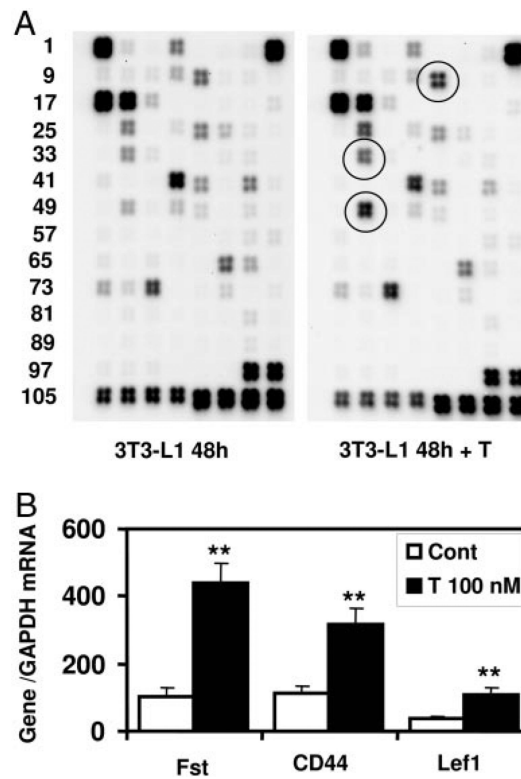
Fig. 7.
Activation of Wnt target genes by testosterone (T). A, Effect of testosterone treatment on Wnt signaling pathway genes in 3T3-L1 cells by SuperArray Analysis. 3T3-L1 cells were allowed to differentiate into AM as described in *Materials and Methods* for 48 h either in presence or absence of testosterone (100 n$_M$). Total RNA was isolated form these cells, and Wnt signaling pathway genes were analyzed by SuperArray as described. *Circled spots* represent some of the listed Wnt target genes, which are up-regulated by testosterone treatment. B, Verification of SuperArray data by quantitative real-time RT-PCR analysis. Total RNA isolated from 3T3-L1 cells after testosterone treatment were analyzed by real-time PCR as described in *Materials and Methods* using gene-specific primers Fst, CD44 and LEF-1 normalized with GAPDH (**, $P < 0.0004$).

Author Manuscript

Author Manuscript

Author Manuscript

Author Manuscript
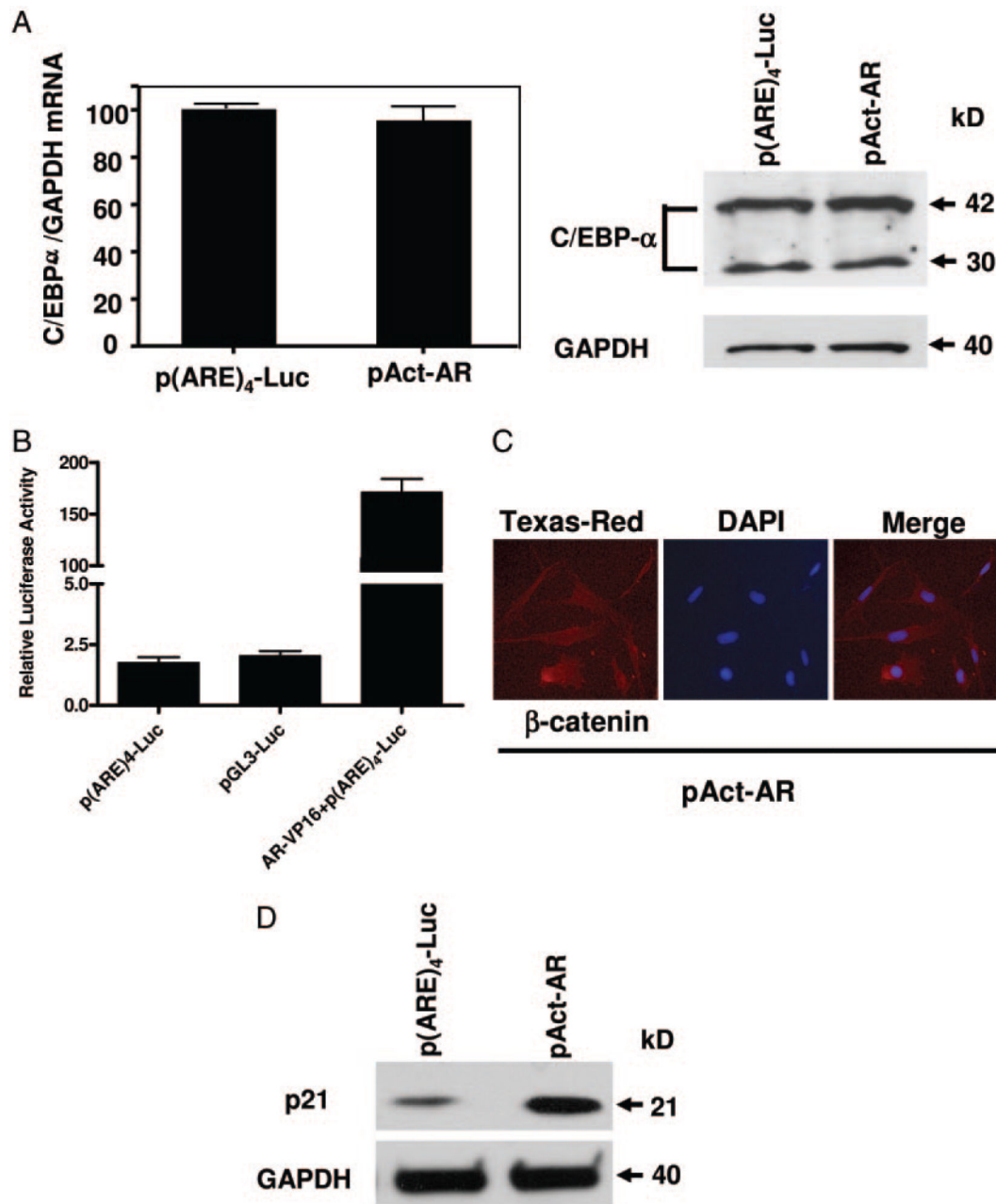
Fig. 8.
Effect of constitutive activation of AR on adipogenesis. A, Expression of C/EBPα mRNA and protein. Cells were transiently transfected either with pAct-AR or pARE4-Luc using Lipofectamine 2000 and allowed to differentiate in adipogenic conditions for 9 d in absence of androgen. C/EBP-α protein and mRNA were analyzed by Western blot (*right*) and real-time RT-PCR (*left*), respectively. Data for real-time RT-PCR (done in quadruplicate for each treatment) and Western blot are from a single experiment representative of three separate experiments. B, Dual-luciferase reporter assay. Cells were transiently transfected with either pGL3, pARE4-Luc alone or pAct-AR in combination with pARE4-Luc and allowed to grow for 2 d in growth medium. Cells were also cotransfected with Renilla

luciferase plasmid pRL-TK-Luc (50:1) using Lipofectamine 2000 and dual-luciferase assay was performed using standard protocols. The relative luciferase activity is presented in arbitrary units as mean ± sd from four separate experiments. C, Immunofluorescence analysis. Cells plated on two-well chamber slides were transiently transfected with pAct-AR, fixed with 2% paraformaldehyde, and immunofluorescence was performed using anti-β catenin antibody (Texas Red). D, Expression of p21 protein. Cells were transiently transfected either with pARE$_4$-Luc or pAct-AR as described in panel A and allowed to differentiate in adipogenic medium for another 2 d. Cells were lysed, and p21 expression was analyzed using anti-p21 antibody.

TABLE 1 Wnt target genes and expression profile

Super Array MM-043, relative gene expression					
Gene no.	Unigene no.	Gene name	Con^a	Test^b	Test/Con
13. Cd44	Mm.330428	CD44 antigen	25593	57496	2.2
34. Fst	Mm.4913	Follistatin	12605	29014	2.3
50. Lef1	Mm.255219	Lymphoid EB factor 1	8064	38388	4.8

Real-time RT-PCR, relative gene expression					
PCR primer	GenBank accession no.	DNA (bp)	Con^c	Test	Test/Con
Cd44	NM_009851	183	110	314	2.8
Fst	NM_008046	150	100	442	4.4
Lef1	NM_010703	132	37	108	2.9

^{a}Intensity minus blank for control (Con).

^{b}Intensity minus blank for testosterone normalized by 1.7.

^{c}Average gene/average GAPDH, normalized to Fst control.